DENTAL MATERIALS 35 (2019) 105–113

Available online at www.sciencedirect.com

ScienceDirect

journal homepage: www.intl.elsevierhealth.com/journals/dema

Influence of glass-ceramic coating on composite zirconia bonding and its characterization

Putsadeeporn Thammajaruk[a,*], *Supanee Buranadham*[b], *Ornnicha Thanatvarakorn*[c], *Marco Ferrari*[d], *Massimiliano Guazzato*[e]

[a] *Department of Bioengineering, Sydney Dental School, Faculty of Medicine and Health, The University of Sydney, Westmead, NSW, 2145, Australia*
[b] *Department of Prosthetic Dentistry, Prince of Songkla University, Songkhla, 90110, Thailand*
[c] *Department of Operative Dentistry, Bangkokthonburi University, Bangkok, 10170, Thailand*
[d] *Department of Prosthodontics and Dental Materials, University of Siena, Siena, 53100, Italy*
[e] *Department of Prosthodontics, Sydney Dental School, Faculty of Medicine and Health, The University of Sydney, Westmead, NSW, 2145, Australia*

ARTICLE INFO

Article history:
Received 25 May 2018
Received in revised form
24 October 2018
Accepted 1 November 2018

Keywords:
Ceramic
Zirconia
Resin cement
Micro-tensile bond strength
Fourier Transform Infrared Spectroscopy (FTIR)

ABSTRACT

Objective. The aims of this study were to compare micro-tensile bond strength and characterize the bond of ceramic-coated versus air-abraded and chemically treated zirconia specimens.

Methods. Eight zirconia blocks were fabricated and assigned to two groups as follows: AA-alumina air-abrasion; and CC-DCMhotbond coating followed by alumina air-abrasion and hydrofluoric acid etching. For each group, two identically pre-treated zirconia blocks were applied G-Multi Primer, cemented together with G-Cem Linkforce cement and cut into 30 stick-shaped specimens ($1 \times 1 \times 9\,mm^3$). A total of 120 specimens were stored in distilled water for 24 h and then assigned to three groups: (i) short-term test, (ii) thermocycling for 5000, and (iii) thermocycling for 10,000 cycles. The specimens were tested in tensile mode. The bond strength results were analyzed using two-way ANOVA, followed by one-way ANOVA and Dunnett T3 ($\alpha = 0.05$). Failure mode and surfaces were analyzed with optical microscopy and SEM. The EDS, FTIR, XRD, and FIB-SEM were used for chemical, crystalline phase analyses.

Results. The AA groups recorded higher mean bond strength than the CC groups in all aging conditions. Thermocycling did not affect the bond strength of the AA groups, whereas the bond strength of the CC groups decreased significantly after aging. The MDP monomer and silane in G-Multi Primer chemically reacted with mechanically pre-treated AA and CC surfaces via the absorption of P–O and Si–O groups.

Significance. The bond strength of a conventional protocol involving alumina air-abrasion was greater than ceramic coating technique.

* *Corresponding author at*: Department of Bioengineering, Sydney Dental School, Faculty of Medicine and Health, The University of Sydney, Level 2, Westmead Center of Oral Health, Darcy Road, Westmead, NSW, 2145, Australia.
E-mail address: ptha8204@uni.sydney.edu.au (P. Thammajaruk).
https://doi.org/10.1016/j.dental.2018.11.001

1. Introduction

Zirconia restorations have become increasingly popular owing to their superior mechanical properties when compared to glass-ceramics [1,2]. Due to the lack of a glassy matrix, zirconia based ceramics can neither be etched by hydrofluoric acid (HF) to increase the surface roughness nor utilize the application of a silane to enable the bond with silica and copolymerize with organic resin matrix in resin cements [3,4]. Improving the bond strength and durability of zirconia to resin cements and tooth structure would contribute to the expansion of its clinical applications in regions where adequate bonding areas and mechanical retention are limited.

Various methods to promote bonding between zirconia and resin cements have been proposed [5,6]. One of the most common protocols to achieve sufficient clinical bond strength between zirconia and resin cement is based on the preparation of zirconia with alumina air-abrasion followed by adhesive primer containing 10-methacryloyloxydecyl dihydrogenphosphate (10-MDP) [7]. Previous studies supported the use of MDP to increase bonding strength between zirconia and resin cement [8,9] via the formation of chemical bond [10]. The use of air abrasion favors bonding by increasing surface area and roughness. On the contrary, alumina air-abrasion may affect mechanical properties of zirconia by creating surface flaws and triggering tetragonal to monoclinic ($t-m$) phase transformation [11,12].

Alternative zirconia-conditioning techniques, based on ceramic coating, have been developed with the purpose of achieving a chemically reactive surface where a primer can be used to create a strong bond to resin cement [13]. A recent in vitro systematic review and meta-analysis of bonding to zirconia appeared to indicate that ceramic coating, combined with MDP containing primers, yielded the greatest long-term bond strength (in aged-condition) comparing to the other pre-treatment techniques [14]. The greatest bond strength of this pre-treatment may be attributed to the silica composition of the coating layer on zirconia surface, which can be etched and primed. The glass-ceramic coating layer can be created with different techniques e.g. selective infiltration etching [15], glazing techniques [16,17], ceramic liner [6], and bioglass [18]. Despite the encouraging bond strength data, there is limited evidence supporting the chemical affinity between the ceramic-coated zirconia surface and the primer and documenting the bonding efficacy between these materials [19]. Furthermore, some studies reported a thickness of the coating layer ranging from 47 to 271 μm. Such thickness may negatively impact on the fitting of the restorations [17,18].

Recently, a novel ceramic coating (DCMhotbond coating) technique has been introduced. This technique relies on the formation of an evenly thin (under 20 μm) layer of glass, which is sintered on the fitting surface. After sintering, this coating layer is air-abraded with alumina particles, HF etched and then primed prior to cementation with resin cement. The use of this material and protocol simulate the bonding of conventional glass-ceramics and it is supposed to be superior in strength and durability to bonding techniques based on mechanical and chemical preparation of the zirconia surface, as above-mentioned.

The aims of this study were to compare the micro-tensile bond strength to resin cement of ceramic-coated and air-abraded zirconia which were chemically treated by MDP and silane containing primer and to characterize the nature of the bond. The null hypotheses tested were: (1) there was no significant difference in bond strength between the new ceramic coating technique and a conventional technique based on alumina air-abrasion, and (2) thermocycling would not affect the bond strength in both tested groups.

2. Materials and methods

2.1. Specimen preparation and mechanical surface pre-treatment

Eight zirconia blocks ($13 \times 26 \times 5.9\,mm^3$) were fabricated from pre-sintered zirconia disks (GC Initial Zirconia HT Disk, GC Europe N.V., Leuven, Belgium) by a computer-aided design/computer-aided manufacturing (CAD/CAM) process and using a milling machine (Roland DWX-50, Roland DG Corp., Shizuoka-ken, Japan). Following milling, the zirconia blocks were sintered in a furnace (Vita Zyrcomat® 6000MS, Vita Zahnfabrik, Bad Säckingen, Germany) for 2 h at 1450 °C as recommended by the manufacturer. After sintering, the zirconia blocks ($10 \times 20 \times 4.5\,mm^3$) were ultrasonically cleaned for 10 min in acetone and distilled water, respectively. The blocks were then randomly and equally assigned to two groups, named CC (ceramic coating) and AA (alumina air-abrasion). One of the largest surfaces of the blocks of group CC was air-abraded with 105 μm alumina particles at 0.2 MPa for 20 s as recommended by the manufacturer (at a distance of 25 mm between the tip of blasting device and zirconia, angle to the surface around 60°–80°) followed by ultrasonic cleaning in ethanol and then distilled water for 2 min. Ceramic coating (DCMhotbond® Zirconnect powder, Dental Creativ Management GmbH, Rostock, Germany) mixed with a carrier liquid (DCMhotbond® carrier) (0.6 g powder and 3 ml of liquid) was sprayed with an airbrush by pistol (0.15 MPa, at a distance of 10 mm) on the air-abraded zirconia surfaces. DCMhotbond® Zirconnect is a glass based on silica material (SiO_2, Al_2O_3, K_2O, Na_2O, CeO_2, P_2O_5, ZnO, SrO, La_2O_3, and SnO_2) with a coefficient of thermal expansion coefficient of $9.7 \times 10^{-6}\,K^{-1} \pm 0.5$ (25–500 °C). The ceramic coating was dried at 450 °C for 2 min and then heated at 1000 °C for 1 min and cooled to room temperature. The heating and cooling rates (60 °C/min) were programmed in a Programat P300 furnace (Ivoclar-Vivadent, Schaan, Liechtenstein). After cooling, the coated surfaces were air-abraded with 105 μm alumina particles at 0.1 MPa for 20 s (at a distance of 25 mm, angle to the surface around 60°–80°), ultrasonically cleaned with distilled water for 2 min, etched with HF acid gel (4.5%) (Ivoclar Vivadent, Schaan, Liechtenstein) for 20 s, then rinsed with distilled water and air-dried.

One of the largest surfaces of the blocks of AA group was air-abraded as manufacturer's recommendation with 50 μm alumina particles at 0.25 MPa, 10 mm distance, angle to the surface at approximately 90°, for 40 s followed by ultrasonic cleaning with ethanol and distilled water, respectively for 2 min.

2.2. Micro-tensile bond strength (μTBS) test

Before cementation, the mechanically pre-treated surface of both groups was conditioned with MDP and silane-containing primer (G-Multi Primer, GC Corp., Tokyo, Japan). Two identically pre-treated zirconia blocks were bonded together using resin cement (G-CEM LinkForce, GC Corp., Tokyo, Japan) under a constant load of 750 g. Excess cement was removed with cotton pellets. Light polymerization was initiated with a halogen light curing unit (Optilux 501, Kerr Corp., CA, USA) for 20 s (output of 850 mW/cm^2) on each side from 6 different sides of the bi-layered zirconia blocks, followed by self-curing for 10 min.

Each bi-layered zirconia block was sectioned into stick-shaped specimens with an approximately cross-sectional area at the bonding interface of 1.0 × 1.0 mm^2 by using a water-cooled diamond saw (Isomet 4000, Buehler, IL, USA) at low speed (600 rpm, feed rate 4 mm/min). Thirty microbars from the center of each zirconia block were selected (n = 60/group).

All specimens were stored in distilled water at 37 °C for 24 h, then the specimens were equally assigned to 3 aging conditions (N = 20/group): (i) short-term, [20] (ii) thermocycling for 5000 cycles between 5 °C (+/−2 °C) and 55 °C (+/−2 °C) with 30 s dwell time and 10 s transfer time, and (iii) thermocycling for 10,000 cycles.

After designated aging period, the specimens were subjected to μTBS with a universal testing machine (LRX-Plus, Lloyd Instrument Ltd., Hampshire, UK) at a speed of 1 mm/min until failure occurred. The Shapiro–Wilk test indicated that the normality assumption for the bond strength data was satisfied. The bond strength data were statistically analyzed using two-way ANOVA followed by one-way ANOVA and Dunnett T3 as post hoc comparisons. All statistical analyses were performed at 0.05 significant level ($\alpha = 0.05$) with software (IBM SPSS statistics V24.0, IBM Corp., NY, USA). In case of pre-treatment failure, 0 MPa was assigned to the bond strength value and included in the statistical analysis.

2.3. Failure mode analysis

The fractured specimens were observed under a light microscope (Olympus BX 60, Olympus Corp., Tokyo, Japan) at 50× magnification and a field emission scanning electron microscope (FE-SEM, Zeiss Sigma VP FEG SEM, Carl Zeiss Microscopy GmbH, Jena, Germany) to identify the type of failure, as follows [21]:

Group AA

- Type 1: adhesive failure (80%–100% of failure occurred at the interface between zirconia and resin cement).
- Type 2: cohesive failure (80%–100% of failure occurred inside resin cement or zirconia).
- Type 3: mixed failure (mixed with adhesive and cohesive failure patterns in the same specimen).

Group CC

- Type 1: adhesive failure (80%–100% of failure occurred at the interface between resin cement and ceramic coating, or ceramic coating and zirconia).
- Type 2: cohesive failure (80%–100% of failure occurred inside resin cement, zirconia, or ceramic coating layer).
- Type 3: mixed failure (mixed with adhesive and cohesive failure patterns in the same specimen).

2.4. Weibull statistics

The μTBS data were analyzed by Weibull distribution (Minitab Software V.18, State College, PA, USA). Pre-treatment failure data were excluded. Weibull parameters (Weibull characteristic strength at 63.2% probability of failure and Weibull modulus) were computed by maximum-likelihood estimation whereas 95% confidence intervals (CIs) were calculated with Parametric Distribution Analysis (Right Censoring). The significant difference in test groups was compared using Weibull parameters and 95% CIs.

2.5. Morphology of pre-treated surfaces

An additional block from each group was observed with a FE-SEM at 1000× to assess surface topography following mechanical pre-treatment.

2.6. Chemical characterization

Elemental composition of as sintered zirconia, and ceramic coating (without alumina air-abrasion and HF etching), the mechanically pre-treated CC and AA surfaces with and without primer conditioning was analyzed using an Energy Dispersive X-ray Spectroscopy (EDS) (EDS Software-AZtecEnergy, Oxford Instruments, High Wycombe, UK).

Infrared spectra were collected using Fourier-Transform Infrared (FTIR) spectrometer (Bruker ALPHA portable spectrometer, Bruker, Karlsruhe, Germany) equipped with a single reflection diamond attenuated total reflection (ATR) module and deuterated triglycine sulphate (DTGS) detector. Spectra were collected on primer alone (as a reference) and the primed CC and AA mechanically pre-treated surfaces at ambient condition over the region of 300–4000 cm^{-1} with resolution of 4 cm^{-1}, 256 sample scans and air background. Range between 860 and 1270 cm^{-1} was fitted using pseudo-Voigt function with a constant profile factor of 0.5.

2.7. Phase transformation analysis

As sintered zirconia, ceramic-coated zirconia (without alumina air-abrasion and HF etching), the mechanically pre-treated CC and AA surfaces were examined by X-ray Diffraction (XRD, Diffractometer D5000, Siemens, Karlsruhe, Germany) to quantify the relative amount of monoclinic phase. XRD data were collected with Cu Kα radiation from 25 to 35° 2θ degrees with a step size of 0.02° and with a 1 s step interval. The equation suggested by Garvie and Nicholson was used to calculate the relative amount of monoclinic phase [22].

The depth of the $t - m$ transformed layer was investigated by focused ion beam scanning electron microscope (FIB-SEM) (Zeiss Auriga FIB-SEM, Carl Zeiss Microscopy GmbH, Jena, Germany) following mechanical pre-treatment. Additionally, the thickness of ceramic coating layer was measured by FIB-SEM.

Table 1 – The results of bond strength, Weibull analysis and the recorded failure mode.

Group	Storage	Bond strength[1,2]	M[3]	B 63.2%[3]	Failure analysis		
					Ad[4]	Co[5]	Mixed
AA	24 h	90.88 (17.41)aA	6.14 (4.34–8.69)XZ	97.95 (90.84–105.61)P	35%	–	65%
	TC 5000	90.12 (8.54)aB	11.67 (8.45–16.10)X	93.88 (90.21–97.68)P	30%	5%	65%
	TC 10,000	80.29 (23.37)aC	3.94 (2.80–5.57)YZ	88.83 (78.99–99.89)P	35%	5%	60%
CC	24 h	37.57 (9.90)xD	4.31 (3.07–6.06)YZ	41.31 (37.10–56.00)Q	–	95%	5%
	TC 5000	24.05 (3.06)yE	8.64 (6.22–11.99)X	25.38 (24.06–26.79)R	–	100%	–
	TC 10,000[6]	13.43 (7.93)zF	3.15 (2.13–4.66)YZ	17.70 (15.11–20.74)S	–	100%	–

TC: thermocycling between 5 °C (+/–2 °C) and 55 °C (+/–2 °C) with 30 s dwell time and 10 s transfer time.
[1] Different lower-case letters in one column indicate significant differences among aging conditions in the same group.
[2] Different upper-case letters in one column indicate significant difference between AA and CC in each aging condition.
[3] Different upper-case letters in one column indicate significant difference among group (no overlapping).
[4] Ad: adhesive failure.
[5] Co: cohesive failure in ceramic coating.
[6] ptf: pre-treatment failure 3 pieces (15%).

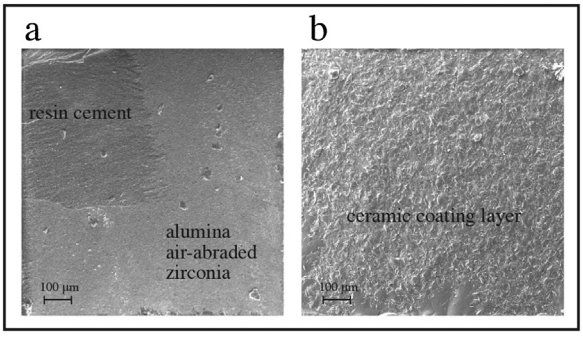

Fig. 1 – SEM images illustrating the fracture surface of AA and CC specimens: (a) mixed failure of AA specimen: (b) cohesive failure in ceramic coating layer of CC specimen.

3. Results

3.1. Micro-tensile bond strength (μTBS) test

Means and standard deviations (SD) of the μTBS of CC and AA groups under 3 aging conditions are presented in Table 1. The mean μTBS of AA groups was significantly higher than CC groups for all aging conditions ($p < 0.05$). Thermocycling did not affect the μTBS of AA groups ($p > 0.05$), whereas μTBS significantly decreased in CC groups ($p < 0.05$).

3.2. Failure mode analysis

Most of the CC specimens exhibited predominantly cohesive failure in ceramic coating layer, whereas almost all specimens in AA groups presented either mixed or adhesive failure, regardless of aging conditions (Table 1 and Fig. 1)

3.3. Weibull analysis

The Weibull parameters are shown in Table 1. Weibull characteristic strength for AA groups was greater than CC groups (in any aging condition). The Weibull modulus values of AA and CC groups were not statistically significantly different when compared in each aging condition.

3.4. Morphology of pre-treated surfaces (SEM)

SEM images of mechanically pre-treated CC and AA surfaces are shown in Fig. 2. Images of the mechanically pre-treated AA surface showed the typical abraded topography, whereas the CC surface showed the presence of long and thin cracks ($20 \times 0.3\ \mu m^2$) in the ceramic coating layer.

3.5. Chemical characterization (EDS and FTIR)

The percentage of elements composition on as sintered zirconia, pre-treated zirconia surface: alumina air-abrasion, ceramic coating (without alumina air-abrasion and HF etching), and ceramic coating followed by HF etching (with and without primer application) are shown in Appendix Table A1. Zr and O were the major elements found on as sintered zirconia and the mechanically pre-treated AA surfaces whereas O and Si were mainly detected in ceramic-coated zirconia and for the mechanically pre-treated CC group. Upon primer application, higher percentage of P and C was detected. EDS maps of mechanically pre-treated zirconia surface: alumina air-abrasion and ceramic coating followed by HF etching are showed in Fig. 3.

Collected FTIR spectra are shown in Fig. 4 and fitting parameters are given in Appendix Table B1. FTIR spectra of both primed specimens exhibited spectral broadening and increase of integrated peak area when, compared to the primer. The most prominent difference between the spectra of primer and primed specimens was the split of the 977 cm^{-1} primer peak into higher and lower wavenumber components, i.e. 965 and 983 cm^{-1} in primed CC specimen versus 955 and 985 cm^{-1} in primed AA.

3.6. Phase transformation analysis (XRD and FIB-SEM)

XRD analysis quantified the percentage of monoclinic phase transformation of as sintered zirconia as 3.02%, for ceramic-coated zirconia as 0% and for the mechanically pre-treated CC surface as 3.19%, whereas it was 5.43% for AA. FIB-SEM showed the cross-sections of the mechanically pre-treated CC and AA surfaces (Fig. 2) as well as the $t - m$ transformed layer depth

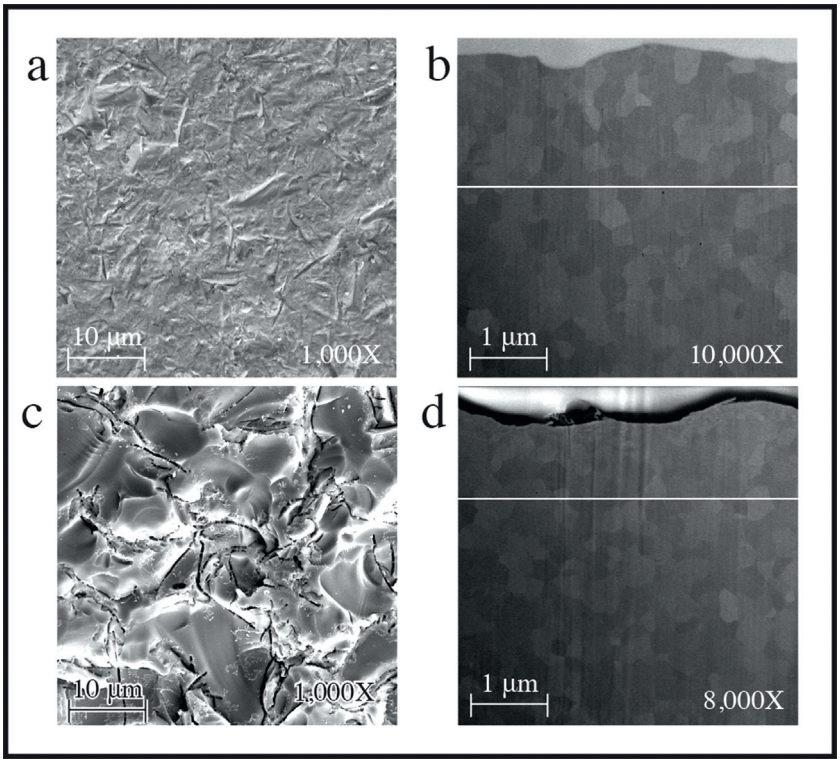

Fig. 2 – Surface topography of mechanically pre-treated zirconia surface using FE-SEM and cross-sectional surface topography of mechanically pre-treated zirconia surface using FIB-SEM: (a, b) alumina air-abrasion: and (c, d) ceramic coating followed by HF etching. The white line indicated an estimate of the *t* – *m* transformed layer border.

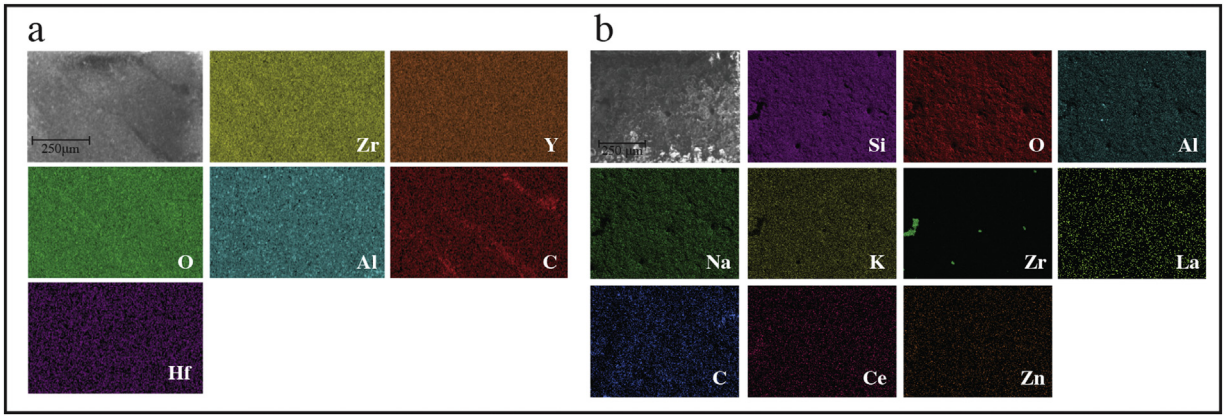

Fig. 3 – EDS maps of mechanically pre-treated zirconia surface: (a) alumina air-abrasion: and (b) ceramic coating followed by HF etching.

of approximately 1.93–2.75 μm and 2.57–3.14 μm, respectively. The thickness of ceramic coating layer as measured by FIB-SEM ranged from 6.9 to10.8 μm.

4. Discussion

The results of this study showed that CC groups yielded significantly lower bond strength than AA groups for all aging conditions. Thus, the first hypothesis was rejected. After thermocycling, μTBS of CC groups significantly decreased; however, thermocycling did not affect the bond strength of AA groups. Therefore, the second hypothesis was partially accepted.

The use of alumina air-abrasion followed by chemical treatment with MDP containing primer and cementation with resin cement has been widely accepted as an effective technique for cementation of zirconia-based restorations [7]. Air abrasion increases surface roughness, surface energy and facilitate wettability which contribute to micromechanical retention of resin cement to zirconia surface [23], whereas MDP monomers promote chemical bond to the oxide group of zirconia [10]. Several studies have confirmed the effectiveness of the bond between resin cement and zirconia with this technique [24,25].

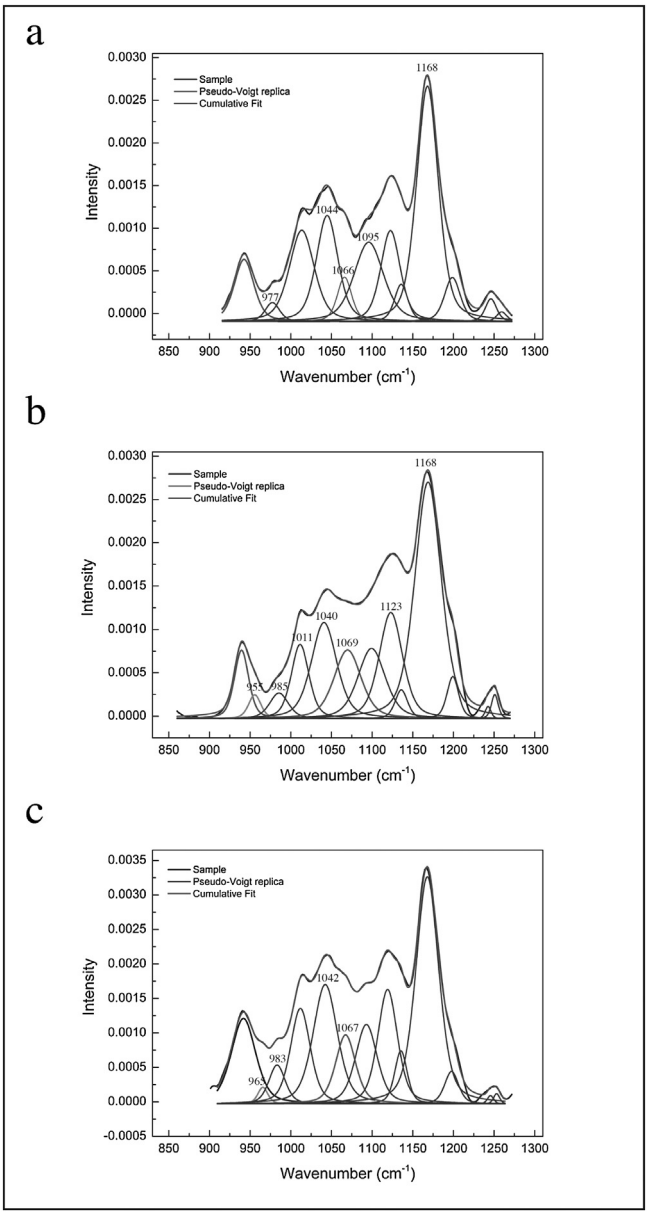

Fig. 4 – FTIR transmittance spectra of pre-treated zirconia surface and primer: (a) G-Multi Primer: (b) alumina air-abrasion followed by G-Multi Primer: (c) ceramic coating followed by HF etching and G-Multi Primer.

However, some researchers demonstrated decrease in bond strength after long-term aging [26], casting doubts about long-term clinical effectiveness of the bond.

Alternative bonding techniques based on coating zirconia with glass-ceramics to allow HF etching and silanization have been proposed to improve bonding strength and durability [13,16]. The present study investigated one of those techniques, namely DCMhotbond. The main concerns with these novel techniques are thickness of the coating layer, bond strength and durability. EDS confirmed the presence of Si on coated zirconia surface, while FIB-SEM showed the presence of ceramic coating layer with thickness of approximately 6.9–10.8 μm. Such thickness is less than what reported in previous studies and should not affect fitting of the restorations [16,17]. In addition, HF etching and silanization of the ceramic layer was expected to contribute to greater bond strength [5,13,27]. However, the present study showed that CC groups possessed significantly lower immediate μTBS than AA groups. The SEM images of the etched ceramic-coated zirconia surface showed the presence of long cracks with a width of less than 1 μm on coating layer. The width of the cracks is unlikely to allow for the infiltration of the filler particles of resin cement into these irregularities, leading to poor micromechanical interlocking. Whilst the length and depth of the cracks is expected to weaken the coating layer and cause cohesive failure within the coating layer as observed in CC groups. Furthermore, thickness of the coating layer was not consistent. EDS maps revealed that in some areas zirconia was exposed (Fig. 3). The presence of areas where zirconia was exposed, was consistently seen in all mechanically pre-treated CC specimens and also in the pilot study. A bonding system which contained MDP and silane (G-Multi Primer, GC Corp., Tokyo, Japan) was selected to maximize the bonding effectiveness to the zirconia and glass-coating system.

FTIR spectra of primed CC specimen bore more resemblance to the primer than primed AA, which was an indicator of better structural interaction between primer and mechanically pre-treated AA specimen than in the case of CC (Fig. 4 and Appendix Table B1).

The most prominent difference between the spectra of primer and primed specimens was the split of the 977 cm^{-1}. This split indicates that priming reduced the size and number of phosphate units in large metaphosphate rings, i.e. $(PO_4)^{3-}$. These metaphosphate rings are partly involved in bonding with the substrate [28,29]. Additional peaks at 955 and 965 cm^{-1} in primed CC and AA specimens spectra could be attributed to the P—O—Al bonding [30]. Comparison of reduced intensities ($I_{iR} = I_i/\Sigma I$) revealed that the $I_R(955)/I_R(985)$ in primed AA specimen was considerably higher than $I_R(965)/I_R(983)$ in primed CC specimen, indicating an increase of the mixed P—O—Al bonding in primed AA. Stretching of polymerized $(PO_4)^{3-}$ species, observed in primer at 1044 cm^{-1}, shifted to 1042 and 1040 cm^{-1} in primed CC and primed AA specimens, respectively, due to an interaction with Si and Al on specimen surfaces. Peaks observed at 1066 cm^{-1} in primer and 1067 cm^{-1} in primed CC specimen could be assigned to the Si—O bond [31]. The broadening and intensifying of this peak could be understood in terms of an increase in siloxane bonds in primed CC specimen. However, siloxane bond detected in primed CC specimen may possess low hydrolytic stability, which leads to a decrease in bond strength after aging [32,33].

In primed AA specimen, the increase of 1069 cm^{-1} Si—O component was followed by the decrease in intensity of peaks associated with uniformly bonded $(PO_4)^{3-}$ species at 1011 and 1040 cm^{-1}. Additionally, a shift of $(PO_3)^{2-}$ related peak at 1095 cm^{-1} in primer towards the $(PO_2)^{-}$ region at 1123 cm^{-1} and the increase in intensity of $(PO_2)^{-}$ terminal group indicate better mixing between alumina and phosphate in primed AA specimen.

These observations point to the conclusion that priming reduces the size of the metaphosphate rings and redistributes the population of terminal phosphate species as they become bonded with additional phases, namely Si and Al.

When Weibull analysis is applied to bond strength studies, the greater the Weibull characteristic strength, the better the actual bonding effectiveness; and the greater the Weibull modulus, the less the bonding procedure is technique sensitive [34]. Greater Weibull characteristic strength values reported for the AA groups under any aging condition showed that the bonding effectiveness was greater than that of the CC groups. However, the Weibull modulus values of AA and CC groups were not statistically significantly different when compared in each aging condition, implying that the technique sensitivity of both groups was similar.

XRD analysis measured a lower amount of $t-m$ phase transformation in the CC group than in the AA group. Different pressure and particles size were used for groups CC and AA. This result appears to indicate that higher air pressure used for treating the AA group, compared to that used for CC group, may contribute to a greater amount of phase transformation, regardless of the particle size used for air abrasion (smaller in the group AA). However, the sensitivity of XRD analysis is limited by the depth of penetration of the X-rays, which might not exceed 6–10 μm [35,36]. In this study, the thickness of the ceramic coating layer (0–10.8 μm) might have hindered the measurement. Due to these limitations, the depth of the $t-m$ phase transformation was investigated by FIB-SEM. In FIB-SEM images, the transformed zone exhibits as a smoother surface with twinning grain boundaries, which allows direct measurement of the transformed layer [37]. In present study, the depth of the $t-m$ transformed layers as measured by FIB-SEM ranged from 1.93 to 2.75 in group CC and from 2.57 to 3.14 μm in group AA, confirming that the *t-m* phase transformation was greater and deeper in the AA group.

5. Conclusions

Within the limitations of this study, it can be concluded that type of pre-treatment technique affected the mean bond strength between resin cement and zirconia, as alumina air-abrasion combined with G-Multi Primer and G-Cem Linkforce (AA) showed significantly higher bond strength than DCMhot-bond coating technique followed by G-Multi Primer and G-Cem Linkforce (CC) for all aging conditions. Thermocycling did not affect the bond strength of AA groups whereas the bond strength of CC groups decreased significantly after aging.

The MDP monomer and silane in G-Multi Primer chemically reacted with the mechanically pre-treated AA and CC surfaces via the absorption of P–O and Si–O groups.

Acknowledgements

This study was supported by the Australian Dental Research Foundation Inc., [grant no. RC/PC: E1405/RP549) and GC Corp. [grant no. RC E1512, Project no. D1387]. The authors are grateful to Mrs. Chanya Chuenarrom for her technical assistance in laboratory preparation. The authors acknowledge GC Corp. for supplying the materials used in this study. The authors also acknowledge Dr. Anna-Maria Erika Welsch for FTIR analysis as well as the facilities, scientific and technical assistance from the staff in the Vibrational Analytical and Australian Microscopy and Microanalysis Research Facility (ammf.org.au), The University of Sydney. Dr. Putsadeeporn Thammajaruk gratefully acknowledges the Office of Higher Education Commission, Thailand, for the Strategic Scholarships Fellowships Frontier Research Network (Specific for Southern region).

Appendix A.

Table A1 – Percentage of elements composition on as sintered zirconia, pre-treated zirconia surface: alumina air-abrasion (with and without primer application), ceramic coating (without alumina air-abrasion and HF etching), and ceramic coating followed by hydrofluoric acid (HF) etching (with and without primer application).

Element	As sintered zirconia	Alumina air-abrasion	Alumina air-abrasion followed by G-Multi Primer	Ceramic coating (without alumina air-abrasion and HF etching)	Ceramic coating followed by HF etching	Ceramic coating followed by HF etching and G-Multi Primer
Zr	59.2 (0.1)	59.2 (0.2)	39.3 (0.1)	2.8 (0.6)	1.2 (0)	1.4 (0.1)
O	30.5 (0.1)	28.5 (0.1)	29.9 (0.1)	44.1 (0.3)	46.8 (0.1)	39.8 (0.2)
Y	1.0 (0)	2.5 (0.1)	1.9 (0)	–	–	–
Hf	0.8 (0)	1.3 (0.1)	0.4 (0)	–	–	–
C	8.4 (0.1)	7.1 (0.2)	25.9 (0.1)	4.2 (0.6)	8.3 (0.2)	29.6 (0.3)
Al	0.1 (0)	1.4 (0)	1.6 (0)	5.3 (0.1)	5.0 (0)	3.3 (0)
Si	–	–	0.1 (0)	27.3 (0.4)	24.5 (0.1)	16.5 (0.1)
Na	–	–	–	7.5 (0.1)	7.1 (0)	4.5 (0.1)
K	–	–	–	4.6 (0.1)	3.9 (0)	2.6 (0)
La	–	–	–	1.9 (0.1)	1.9 (0)	1.1 (0.1)
P	–	–	0.9 (0)	–	–	0.3 (0)
Zn	–	–	–	1.8 (0.2)	0.8 (0)	0.6 (0)
Ce	–	–	–	0.5 (0.1)	0.5 (0)	0.3 (0)

Appendix B.

Table B1 – Results of curve fitting.

Para-meter	G-Multi Primer	Value	SE	Primed CC specimen	Value	SE	Primed AA specimen	Value	SE
y0	Peak1	−9.11E-05	0	Peak1	−2.79E-05	0	Peak1	−2.79E-05	0
xc	Peak1	942.58646	0.22406	Peak1	941.81756	0.53203	Peak1	939.4575	2.03743
A	Peak1	0.02635	4.94E-04	Peak1	0.05576	0.0019	Peak1	0.0208	0.00506
w	Peak1	28.59879	0.5879	Peak1	35.49005	1.01287	Peak1	20.76808	1.22915
mu	Peak1	0.5	0	Peak1	0.5	0	Peak1	0.5	0
xc	Peak2	977.32936	0.88683	Peak2	965.61862	3.05493	Peak2	955.65628	4.38394
A	Peak2	0.00585	8.53E-04	Peak2	0.0044	0.00437	Peak2	0.00625	0.0059
w	Peak2	20.83233	2.25627	Peak2	14.49283	4.69268	Peak2	17.91302	11.50228
				Peak3	983.10825	1.79917	Peak3	985.43365	3.84942
				Peak3	0.01691	0.00833	Peak3	0.01022	0.00507
				Peak3	23.68871	8.96405	Peak3	27.2848	7.91113
xc	Peak3	1013.51893	1.1542	Peak4	1011.78037	1.00831	Peak4	1011.41377	1.22931
A	Peak3	0.04897	0.00516	Peak4	0.05046	0.0125	Peak4	0.02783	0.01075
w	Peak3	36.14968	1.80509	Peak4	28.72713	3.72161	Peak4	25.63412	4.65199
xc	Peak4	1044.71501	0.9631	Peak5	1042.38585	2.74432	Peak5	1040.84214	3.72487
A	Peak4	0.04922	0.00935	Peak5	0.07739	0.02899	Peak5	0.05171	0.03305
w	Peak4	31.26559	3.52321	Peak5	35.24822	6.36691	Peak5	36.78786	8.93951
xc	Peak5	1066.08708	1.2779	Peak6	1067.37591	2.67808	Peak6	1069.81398	6.17025
A	Peak5	0.01369	0.00807	Peak6	0.03678	0.03733	Peak6	0.03952	0.06253
w	Peak5	20.80848	5.07642	Peak6	29.02087	11.78094	Peak6	39.3551	24.71426
xc	Peak6	1095.86978	4.51805	Peak7	1092.94838	3.26119	Peak7	1099.32902	16.70379
A	Peak6	0.05024	0.02144	Peak7	0.04576	0.03646	Peak7	0.04075	0.10164
w	Peak6	42.72058	10.22195	Peak7	31.3552	12.75063	Peak7	39.666	30.52161
xc	Peak7	1122.58822	11.57394	Peak8	1119.07621	3.93865	Peak8	1123.00844	21.71968
A	Peak7	0.03809	0.04156	Peak8	0.06002	0.04433	Peak8	0.05277	0.05688
w	Peak7	28.23939	6.59455	Peak8	28.51689	9.96931	Peak8	33.99978	21.57658
xc	Peak8	1135.75365	8.88557	Peak9	1135.45654	3.50383	Peak9	1135.92059	9.51529
A	Peak8	0.01071	0.03867	Peak9	0.0177	0.02578	Peak9	0.00758	0.03912
w	Peak8	19.47313	25.34272	Peak9	18.16261	10.86591	Peak9	18.04066	33.87804
xc	Peak9	1168.05995	0.1339	Peak10	1167.8706	0.17275	Peak10	1168.77209	0.82439
A	Peak9	0.11066	0.00193	Peak10	0.13848	0.00315	Peak10	0.13291	0.01267
w	Peak9	31.62295	0.50288	Peak10	33.15127	0.72103	Peak10	38.36342	3.15801
xc	Peak10	1198.70389	0.57453	Peak11	1197.7006	0.95086	Peak11	1199.2414	0.72344
A	Peak10	0.01497	0.00113	Peak11	0.01199	0.00181	Peak11	0.01042	2.62E-03
w	Peak10	22.92202	1.4955	Peak11	20.11473	2.59555	Peak11	16.93492	2.69426
xc	Peak11	1246.08594	12.34728	Peak12	1245.56635	9.70819	Peak12	1242.60754	5.13134
A	Peak11	0.00545	9.21E-03	Peak12	0.00134	2.06E-03	Peak12	0.0015	0.00143
w	Peak11	16.22526	2.16484	Peak12	8.90919	3.54388	Peak12	8.4085	2.59422
xc	Peak12	1259.29892	25.23532	Peak13	1253.08577	2.96432	Peak13	1250.85691	1.772
A	Peak12	0.00205	0.00957	Peak13	0.00163	0.00208	Peak13	0.00348	0.00149
w	Peak12	14.55132	54.15555	Peak13	8.62633	5.88547	Peak13	9.87282	3.52288

y0 = zero point (baseline), xc = position (cm^{-1}), A = intensity, w = full width at half maximum, mu = profile parameter for pseudo-Voigt, SE = standard error.

REFERENCES

[1] Guazzato M, Albakry M, Ringer SP, Swain MV. Strength, fracture toughness and microstructure of a selection of all-ceramic materials. Part II. Zirconia-based dental ceramics. Dent Mater 2004;20:449–56.

[2] Guazzato M, Albakry M, Ringer SP, Swain MV. Strength, fracture toughness and microstructure of a selection of all-ceramic materials. Part I. Pressable and alumina glass-infiltrated ceramics. Dent Mater 2004;20:441–8.

[3] Derand P, Derand T. Bond strength of luting cements to zirconium oxide ceramics. Int J Prosthodont 2000;13:131–5.

[4] Kern M, Wegner SM. Bonding to zirconia ceramic: adhesion methods and their durability. Dent Mater 1998;14:64–71.

[5] Aboushelib MN, Kleverlaan CJ, Feilzer AJ. Selective infiltration-etching technique for a strong and durable bond of resin cements to zirconia-based materials. J Prosthet Dent 2007;98:379–88.

[6] Cheung GJ, Botelho MG. Zirconia surface treatments for resin bonding. J Adhes Dent 2015;17:551–8.

[7] Kern M. Bonding to oxide ceramics-laboratory testing versus clinical outcome. Dent Mater 2015;31:8–14.

[8] Koizumi H, Nakayama D, Komine F, Blatz MB, Matsumura H. Bonding of resin-based luting cements to zirconia with and without the use of ceramic priming agents. J Adhes Dent 2012;14:385–92.

[9] Nakayama D, Koizumi H, Komine F, Blatz MB, Tanoue N, Matsumura H. Adhesive bonding of zirconia with single-liquid acidic primers and a tri-n-butylborane initiated acrylic resin. J Adhes Dent 2010;12:305–10.
[10] Chen Y, Lu Z, Qian M, Zhang H, Xie H, Chen C. Effect of 10-methacryloxydecyl dihydrogen phosphate concentration on chemical coupling of methacrylate resin to yttria-stabilized zirconia. J Adhes Dent 2017;19:349–55.
[11] Zhang Y, Lawn BR, Rekow ED, Thompson VP. Effect of sandblasting on the long-term performance of dental ceramics. J Biomed Mater Res B Appl Biomater 2004;71:381–6.
[12] Garcia Fonseca R, De Oliveira Abi-Rached F, Dos Santos Nunes Reis JM, Rambaldi E, Baldissara P. Effect of particle size on the flexural strength and phase transformation of an airborne-particle abraded yttria-stabilized tetragonal zirconia polycrystal ceramic. J Prosthet Dent 2013;110:510–4.
[13] Valentino T, Borges G, Borges L, Platt J, Correr-Sobrinho L. Influence of glazed zirconia on dual-cure luting agent bond strength. Oper Dent 2012;37:181–7.
[14] Thammajaruk P, Inokoshi M, Chong S, Guazzato M. Bonding of composite cements to zirconia: a systematic review and meta-analysis of in vitro studies. J Mech Behav Biomed Mater 2018;80C:258–68.
[15] Aboushelib MN. Evaluation of zirconia/resin bond strength and interface quality using a new technique. J Adhes Dent 2011;13:255–60.
[16] Vanderlei A, Bottino MA, Valandro LF. Evaluation of resin bond strength to yttria-stabilized tetragonal zirconia and framework marginal fit: comparison of different surface conditionings. Oper Dent 2014;39:50–63.
[17] Everson P, Addison O, Palin WM, Burke FJ. Improved bonding of zirconia substructures to resin using a glaze-on technique. J Dent 2012;40:347–51.
[18] Moezzizadeh M, Nojedehian H, Haghi HV. Effect of bioglass and silica coating of zirconia substrate on its bond strength to resin cement. Dent Mater J 2017;36:54–62.
[19] Qian M, Lu Z, Chen C, Zhang H, Xie H. Alkaline nanoparticle coatings improve resin bonding of 10-methacryloyloxydecyldihydrogenphosphate-conditioned zirconia. Int J Nanomed 2016;11:5057–66.
[20] ISO/TS:11405. Dentistry—testing of adhesion to tooth structure. Geneva, Switzerland, 2015.
[21] Prasansuttiporn T, Thanatvarakorn O, Tagami J, Foxton RM, Nakajima M. Bonding durability of a self-etch adhesive to normal versus smear-layer deproteinized dentin: effect of a reducing agent and plant-extract antioxidant. J Adhes Dent 2017;19:253–8.
[22] Garvie RC, Nicholson PS. Phase analysis in zirconia systems. J Am Ceram Soc 1972;55:303–5.
[23] Blatz MB, Sadan A, Martin J, Lang B. In vitro evaluation of shear bond strengths of resin to densely-sintered high-purity zirconium-oxide ceramic after long-term storage and thermal cycling. J Prosthet Dent 2004;91:356–62.
[24] Shin YJ, Shin Y, Yi YA, Kim J, Lee IB, Cho BH, et al. Evaluation of the shear bond strength of resin cement to Y-TZP ceramic after different surface treatments. Scanning 2014;36:479–86.
[25] Yoshida K, Tsuo Y, Meng X, Atsuta M. Mechanical properties of dual-cured resin luting agents for ceramic restoration. J Prosthodont 2007;16:370–6.
[26] Bömicke W, Schürz A, Krisam J, Rammelsberg P, Rues S. Durability of resin-zirconia bonds produced using methods available in dental practice. J Adhes Dent 2016;18:17–27.
[27] Vanderlei AD, Queiroz JR, Bottino MA, Valandro LF. Improved adhesion of Y-TZP ceramics: a novel approach for surface modification. Gen Dent 2014;62:e22–7.
[28] Moustafa Y, El-Egili K. Infrared spectra of sodium phosphate glasses. J Non Cryst Solids 1998;240:144–53.
[29] Pilo R, Kaitsas V, Zinelis S, Eliades G. Interaction of zirconia primers with yttria-stabilized zirconia surfaces. Dent Mater 2016;32:353–62.
[30] Nieminen M, Niinistö L, Lappalainen R. Determination of P/Al ratio in phosphorus-doped aluminium oxide thin films by XRF, RBS and FTIR. Mikrochim Acta 1995;119:13–22.
[31] Lee CY, Van Le Q, Kim C, Kim SY. Use of silane-functionalized graphene oxide in organic photovoltaic cells and organic light-emitting diodes. Phys Chem Chem Phys 2015;17:9369–74.
[32] Debnath S, Wunder SL, McCool JI, Baran GR. Silane treatment effects on glass/resin interfacial shear strengths. Dent Mater 2003;19:441–8.
[33] Heikkinen TT, Matinlinna JP, Vallittu PK, Lassila LV. Long term water storage deteriorates bonding of composite resin to alumina and zirconia short communication. Open Dent J 2013;7:123–5.
[34] Burrow MF, Thomas D, Swain MV, Tyas MJ. Analysis of tensile bond strengths using Weibull statistics. Biomaterials 2004;25:5031–5.
[35] Hübsch C, Dellinger P, Maier H, Stemme F, Bruns M, Stiesch M, et al. Protection of yttria-stabilized zirconia for dental applications by oxidic PVD coating. Acta Biomater 2015;11:488–93.
[36] Lucas TJ, Lawson NC, Janowski GM, Burgess JO. Phase transformation of dental zirconia following artificial aging. J Biomed Mater Res B Appl Biomater 2015;103:1519–23.
[37] Cattani-Lorente M, Scherrer S, Durual S, Sanon C, Douillard T, Gremillard L, et al. Effect of different surface treatments on the hydrothermal degradation of a 3Y-TZP ceramic for dental implants. Dent Mater 2014;30:1136–46.